The 3D Retinal Capillary Circulation in Pigs Reveals a Predominant Serial Organization

Stéphane Fouquet, Ophélie Vacca, Florian Sennlaub, Michel Paques

The 3D Retinal Capillary Circulation in Pigs Reveals a Predominant Serial Organization

Stéphane Fouquet,[1] Ophélie Vacca,[1] Florian Sennlaub,[1] and Michel Paques[1,2]

[1]Institut de la Vision, Sorbonne Universiteés, UPMC University Paris 06, INSERM, CNRS, Paris, France
[2]Centre Hospitalier National d'Ophtalmologie des Quinze-Vingts, INSERM-DHOS CIC 1423, Paris, France

Correspondance: Michel Paques, Quinze-Vingts Hospital, 28 rue de Charenton, Paris F-75012, France; mp@cicoph.org.

SF and OV are joint first authors.

Submitted: April 24, 2017
Accepted: September 30, 2017

Citation: Fouquet S, Vacca O, Sennlaub F, Paques M. The 3D retinal capillary circulation in pigs reveals a predominant serial organization. *Invest Ophthalmol Vis Sci*. 2017;58:5754–5763. DOI:10.1167/iovs.17-22097

Purpose. To establish a model of the retinal capillary circulation in pigs, which in many aspects is close to the human retina.

Methods. Using high density confocal microscopy image stacks of immunolabeled porcine retinal whole mounts, microvessels close to the optic nerve head were traced in three dimensions. The direction of flow of individual capillaries was deduced from their arteriolar and/or venous connections.

Results. From major arteries, second-order arteries traversed the nerve fiber layer and resolved exclusively into the superficial vascular plexus (SVP), which dichotomized the blood flow between radial peripapillary capillaries (RPCs) on one side and the intermediate (IVP) and deep vascular plexus (DVP) on the other. Each RPC was supplied by one or several capillaries from the SVP and drained to the IVP or DVP. The DVP was a mosaic of approximately 300 to 600 μm wide anastomotic watersheds, each drained by one or two venules connected to major veins. A presumptive direction of flow could be determined for >90% of capillaries. These results suggest a model of the capillary circulation in which the three microvessel layers are serially organized with RPCs are in parallel between the SVP and IVP or DVP.

Conclusions. In the peripapillary retina of pigs, microvascular layers have a serial arrangement, with RPCs emerging from the SVP and draining to the IVP or DVP; hence, connected in parallel of this scheme. The bulk of flow, therefore, traverses the SVP and DVP successively. This organization contributes to the higher oxygen saturation in the SVP and RPCs than in the DVP. Physiopathologic implications of this model regarding retinal diseases are discussed.

Keywords: modelization, retinal vasculature, confocal microscopy

Neuroglial tissues rely on a finely tuned blood flow for supplying metabolites and metabolic signals and for disposal of waste products. Most neurons have little tolerance to ischemia; yet paradoxically, the blood flow of the retina relative to tissue weight is low compared to other tissues.[1] This stresses the importance of an optimally designed angioarchitecture as well as a stringent adaptation of blood flow to local oxygen demand. This is illustrated in the fovea, where the width of the foveal pit closely matches the size of the foveal avascular zone.[2,3] Therefore, understanding the distribution of blood flow within retinal layers is of utmost interest in comprehending retinal physiology and pathology. Establishing a three-dimensional (3D) model of capillary circulation also is necessary for the correct interpretation of hemodynamic studies in humans. However, surprisingly enough there is no comprehensive model of the retinal microcirculation in large eyes.

The holangiotic microcirculation of the mammalian retina usually is described as three parallel layers of microvessels with additional capillaries irrigating the nerve fiber layer.[4,5] Very little is known concerning the actual distribution of capillary flow within this complex network. Using confocal microscopy and 3D reconstruction of the microvessel arborescence on rodent retinas, we previously proposed a 3D model of the distribution of blood flow in the rodent eye.[6] This model suggested a serial organization of the blood flow from the superficial vascular plexus (SVP) to intermediary (IVP) and deep vascular plexus (DVP) with venous drainage emerging essentially from the DVP. The presence of a highly anastomotic DVP provided a straightforward explanation for the deep localization of venous collaterals following experimental retinal vein occlusion (RVO).[7] However, in larger eyes, close to the optic nerve the accumulation of ganglion cell axons elicits an additional microvascular network, the radial peripapillary capillaries (RPCs),[4,5] which modify this scheme to an unknown extent. Few detailed studies of the anatomic disposition of retinal capillaries of large mammals have been reported.[8–12] In vivo fluorescein angiography can resolve individual capillaries close to the vitreoretinal interface, yet does not provide reliable observation of deeper microvessels or of connecting vessels even in confocal mode.[13–15] The recent advent of in vivo imaging systems allowing segmentation of microvessel layers, such as adaptive optics ophthalmoscopy[14] or angio-optical coherence tomography (OCTA),[15–22] renewed the interest in the tridimensional disposition of human retinal microvessels. However, the yet limited resolution of OCTA impairs the analysis of the relationship between the layers. In particular, it is not known

if these layers are arranged serially or in parallel. A serial organization would indicate that the blood flow successively traverses the three layers, while a parallel organization would suggest that each layer possesses its own arteriolar supply and venous drainage. Based on high resolution OCTA findings, a predominantly parallel organization has been suggested.[21] Such a pattern was described as superimposed hammocks. This refers to a vascular disposition in which a capillary bed (the hammock) would bridge the space between arterioles and venules (which would be the "supportive cables" of the hammock). Hence, each microvessel layer (SVP, IVP, DVP) would be one hammock, which would not be connected one to the other. Recently, connecting vessels between retinal microvessels layers were resolved by OCTA[22] paving the way toward an in vivo analysis of the flow distribution between layers, yet the presumed direction of the flow within these connecting vessels was not mentioned.

We performed high density confocal microscopy on immunolabeled retinal whole mounts to determine the tridimensional disposition of microvessels in the pig retina, which in many aspects is close to the human eye,[8] in particular, since it contains a significant amount of RPCs.

Materials and Methods

Freshly enucleated eyes ($n = 2$) obtained from two adult male farm pigs (CIRHYO, Montluçon, France) aged 12 months, sacrificed after experiments not affecting the eye, were provided kindly by the Institut Mutualiste Montsouris-Recherche (Paris, France). All experiments were done in compliance with the ARVO Statement for the Use of Animals in Ophthalmic and Vision Research. Eyes were fixed in 4% paraformaldehyde for 30 minutes, then retinas were separated from the RPE and sclera by cutting around the ora serrata and the optic nerve. Dissected retinas were postfixed by immersion in 4% paraformaldehyde for 30 minutes then washed for 5 minutes in sterile PBS at pH 7.4. PBS was changed by blocking buffer (PBS with 1% BSA, 2% normal goat serum, 0.5% Triton X-100). Tissues were incubated in the blocking buffer for either 4 hours at room temperature or at 4°C overnight, and then in *Bandeiraea simplicifolia* lectin-TRITC conjugate (Sigma L5264; 1:100; Sigma, Fallavier, France) to label the entire vascular network and in monoclonal antibody anti-smooth muscle cell actin (SMA) FITC conjugate (Sigma F3777; 1:200) to identify arteries, diluted in blocking buffer for either 4 hours at room temperature or at 4°C overnight. After three washes in PBS, retinas were flat-mounted with the retinal ganglion cell side facing upwards in Fluorsave reagent (Millipore, Burlington, MA, USA) and stored at 4°C.

Confocal image stacks were acquired close to the optic nerve in the visual streak (Fig. 1) with 25 × NA 1.0 and 40 × NA 1.3 objectives on an Olympus FV1000 microscope equipped with a 488 nm argon ion laser line and a 559 nm diode laser line. Using an automated motorized stage, a series of z-stacks were captured from the vitreoretinal interface to the outer nuclear layer. Each z-stack consisted of optical sections collected at 0.5 (×40 magnification) to 1 μm (×25) increments along the z-plane. Thus, a mosaic of adjacent stacks was imaged automatically over 24- to 72-hour acquisition sessions. The MATL module from Olympus Fluoview software ensured a 10% overlap between each tiles. Automated montage then was done using XuvTools open source software[21] to obtain large field views covering 4 × 4 mm areas. Ad hoc adjustment of brightness compensated the relative dimness of deeper layers.

Capillary tracing through stacks was done manually by 3D navigation in the three axes using Imaris software (Bitplane AG, Zurich, Switzerland). In the subsequent descriptions, the direction parallel to the vitreoretinal interface will be referred to as horizontal and the perpendicular direction as vertical, superficial signifies toward the vitreous, and deep toward the choroid. Orientation in space and arteriovenous differentiation was facilitated by nuclear labeling, by the faint background fluorescence of axonal fascicles, and by the SMA labeling of arteries. Thus, major arteries emerging radially from the optic nerve head were identified easily, as well as the three outermost microvascular layers. By navigating through the stack in the z axis the SVP, IVP, and DVP served as landmarks for estimation of the retina depth. To trace the connections of capillaries from one layer to another, single capillaries emerging from a layer were followed through successive frames in the z axis until they merged in another layer. The direction of flow in a particular capillary was deduced from its connection to arterial or venous networks. For instance, capillaries connected to precapillary arterioles in the SVP were assumed to have a flow centrifugal to the SVP, while those in the DVP were assumed to have a flow directed toward the center of watersheds; that is, toward transverse venules. Indeed, the DVP in pigs had a very similar aspect to that of mice,[6] rats,[7] and humans[10,21]; that is, a mosaic of anastomotic watersheds. Therefore, it was assumed that the DVP had a similar organization of capillaries converging toward central venules. This assumption served as a basis for the adjudication of a flow direction in individual capillaries in the DVP, which was propagated upstream and downstream.

Results

On low magnification images, wide field views of the different capillary planes were obtained (Fig. 1). RPCs were long capillaries (up to half a millimeter in the vitreoretinal plane) parallel to axons, showing lateral connections to adjacent RPCs and vertical capillaries. There was no planar organization of RPCs; instead, the pathway of each RPC was made of a succession of linear segments adjacent to a fascicle of ganglion cell axons (Supplementary Fig. S1). The SVP and DVP were a mosaic of arborescent patterns, the DVP being more anastomotic than the SVP. The IVP showed curved capillary segments 50 to 500 μm long interspersed by cross-sectioned capillaries.

From first-order arteries, second order arteries emerged laterally at a steep angle, and reached the SVP with an oblique path through the nerve fiber layer (NFL). Second-order arterioles were connected exclusively to the SVP (Fig. 2). Indeed, we could not find any connection of second-order arteries with RPCs. Hence, we concluded that the SVP was the exclusive recipient of arterial flow.

Among 56 capillaries emerging from the SVP, 32 were directed toward the RPCs and 22 toward the IVP/DVP. At the very tip of the arborescence of precapillary arterioles in the SVP, a few capillaries were connected to adjacent first- or second-order veins. Thus, the SVP dichotomizes the arteriolar flow between the IVP/DVP on one side and the RPCs on the other.

From their emergence in the SVP, capillaries supplying RPCs had a general vertical or slightly oblique direction, insinuating themselves between axonal fascicles, alternating horizontal and vertical segments. Most RPCs were connected to several supplying and draining capillaries. Tracing of individual RPCs in both directions showed that all RPCs had a dual connection, that is with the SVP on one side, and with the IVP or DVP on the other (Fig. 3). Assuming that the SVP provides the inflow, this asymmetric configuration (i.e., on two different layers) enabled us to determine the direction of flow in individual RPCs (Fig. 3, bottom right). Therefore, the RPCs can be

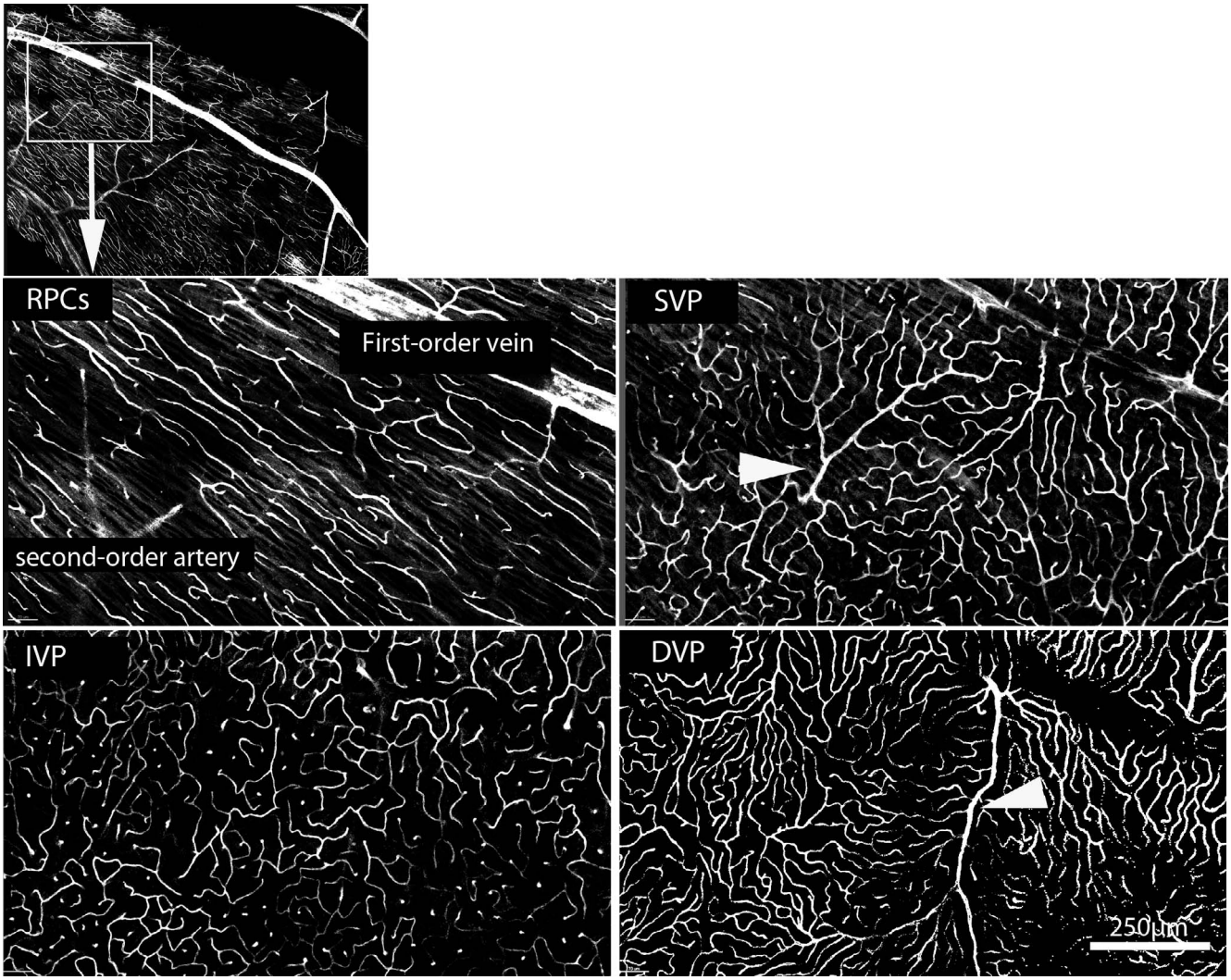

Figure 1. En face view of the different capillary levels of the pig retina close to the optic nerve. In the SVP and DVP, *arrowheads* show a terminal arteriole and a postcapillary venule, respectively.

described as linear capillaries with several feeder capillaries from the SVP and draining into the IVP or DVP. Few RPCs drained directly into neighboring major veins.

Capillaries downward to the SVP either traversed the IVP or, for roughly half of them, horizontally angulated in the IVP. Accordingly, vessels in the IVP comprised capillary segments in the XY plane coexisting with cross-sectioned capillaries and collecting veins. The distribution of the vessels in the IVP was remarkably regular; cross-sectioned capillaries showed similar intervascular spacing as parallel segments (Fig. 4, Supplementary Fig. S2). The mean radius of the capillary-free zone of capillaries (32.2 $\pm$ 12 µm) was smaller than that of transverse veins (50.5 $\pm$ 19 µm; $P < 0.01$).

The DVP was a mosaic of watersheds made of adjacent, anastomotic venous drainage territories, some showing a meandering venules in their center (Fig. 5). Each watershed extended roughly approximately 150 to 300 µm around each transverse venule, which directed venous flow to first- or second-order veins in the inner retina. These transverse veins were approximately 300 to 600 µm distant from each other. Adjacent watersheds were connected by multiple bridging capillaries; hence, it can be postulated that the DVP is anastomotic throughout the entire retina.

Most transverse veins emerging from the DVP traversed the retina with few connections, sometimes after a short oblique path (Fig. 6). They ended under a major vein or second-order veins; they received flow inputs mostly from transverse veins, with a minor contribution from RPCs and SVP.

From the determination of the spatial relationship of each capillary, near-complete maps of the direction of the flow could be established. Indeed, the direction of flow could be presumed in more than 90% of capillaries (Fig. 7). Overall, this suggested that RPCs have no preferential direction of flow, which either would be centripetal or centrifugal relative to the disc. From the quantitative analysis of the microvessel connection, major pathways of flow were deduced and subsequently bi- and tri-dimensional models of the capillary flow direction were built (Fig. 8). The direction of flow in DVP capillaries bridging watersheds could not be determined; indeed, these potentially could carry blood flow in both directions.

Discussion

Here, as an attempt to establish the first detailed model of the distribution of retinal capillary flow in a large mammalian eye,

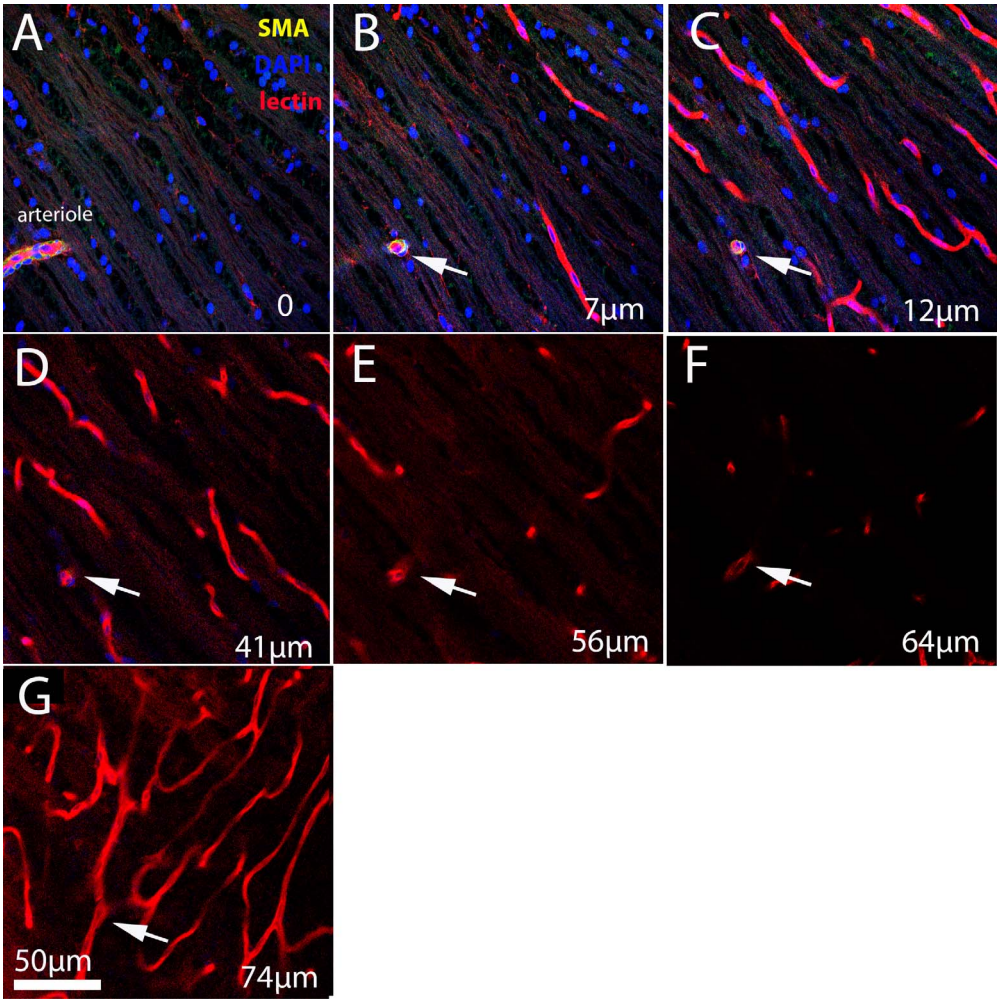

Figure 2. From (**A**) to (**G**), successive images in the *z*-axis of a second-order arteriole (*arrows*) connecting with the SVP (**G**), showing the absence of connection with the RPCs (**B**–**D**). Depth relative to the surface of the retina is indicated. There is no connection between the precapillary arteriole and RPCs.

we analyzed the 3D organization of retinal capillaries in the pig retina in areas showing a thick nerve fiber layer, and, hence, the highest capillary density.[4] Our best-fit model postulates that the bulk of arterial flow irrigates the SVP, which is a crossroads dichotomizing flow to RPCs on one side, and to the serially arranged IVP and DVP on the other. As the flow transiting through RPCs eventually joins the IVP or DVP, we conclude that most of the flow also transits through the DVP. Hence, from the SVP to the DVP there is a dominantly serial organization of the retinal capillary flow. RPCs are connected in parallel of this distributive scheme.

This model closely resembles the one we proposed in the rodent retina,[6,7] which also suggested a predominantly serial organization. The main difference between the rodent and pig retina is the presence of a large amount of RPCs in the pig retina, which renders the latter closer to the human retina. The 3D organization of the outermost microvascular layers also has been approached by Rootman,[12] who proposed a distributive model closely resembling ours yet without the integration of RPCs.

Since the vascular anatomy of the rodents and pig retina has strong resemblances to that of humans, our findings probably have some relevance to humans. The major differences are the presence in humans of a central retinal artery (instead of several cilioretinal arteries in pigs), the deeper location of retinal arteries[7] and the macula with its central avascular zone. Yet, at the level of small vessels there seems to be a remarkable similarity between pigs and humans; close to the human optic nerve, Tan et al.[10] identified four layers of retinal microvessels, the patterns of which were similar to those we found. Also, images of the human DVP obtained by OCTA[22] showed a similar pattern to that we found in pigs. However, in the macula the presences of multilayered retinal ganglion cells and of the foveolar depression fovea are likely to be accompanied by corresponding microvascular adaptation. Thus, the distribution of blood flow in the human macula remains to be understood fully.

Despite the aforementioned differences, our model nevertheless allows some speculations about the physiology and pathology of human retinal microvessels. The oxygen partial pressure varies significantly across neuronal layers.[1,23] The distance between capillaries and the consumption of oxygen determines the relative oxygen content in the immediate environment of each capillary, which may be conceptualized as a cylinder around capillaries (Krogh's cylinder[24]) although this concept suggests a normoxic/anoxic frontier instead of a continuum. Nevertheless, within a specific layer (i.e., within a given neuronal population) it can be assumed that the distribution of microvessels is paralleled by the local oxygen content and, hence, that the intercapillary distance is a

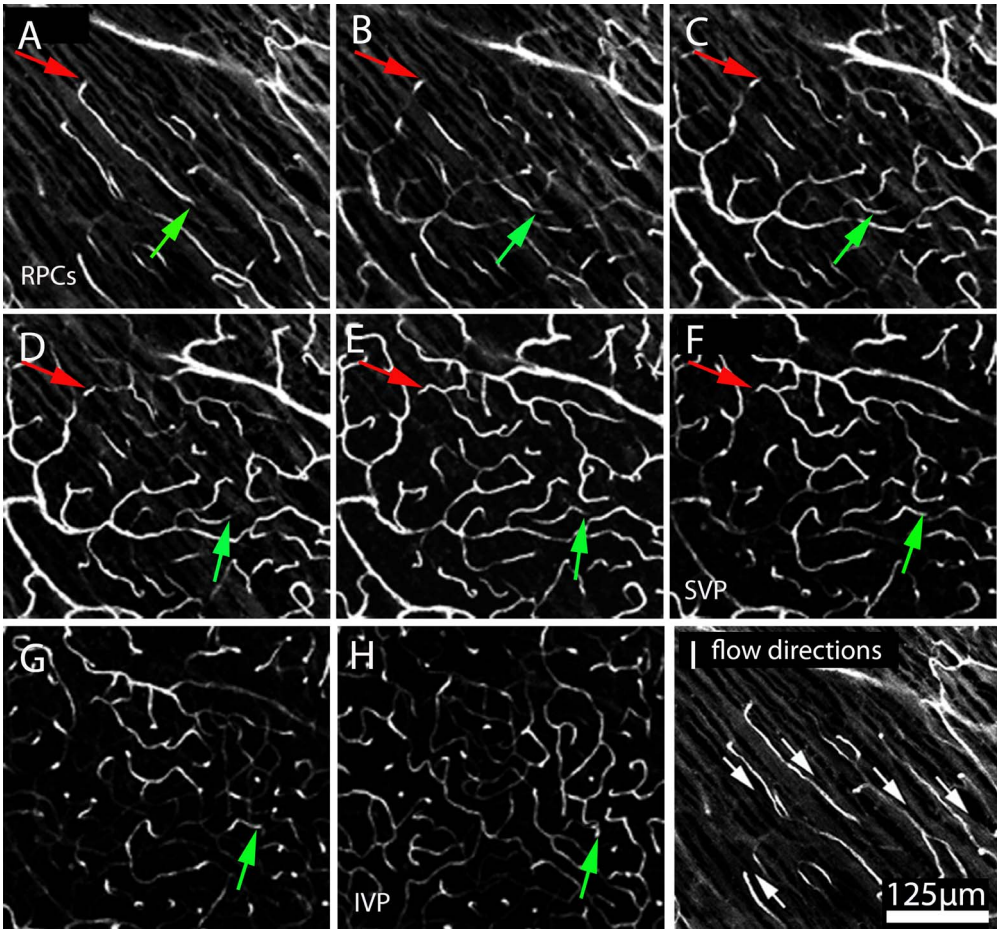

FIGURE 3. From (**A**) to (**H**), illustration of the asymmetric connection of RPCs. The *red arrows* follow an RPC (**A**) to the SVP (**F**), while the *green arrows* trace it to the IVP (**H**). (**I**) Presumed direction of flow in RPCs (same image as *top left*) deduced from their respective connections upstream and downstream.

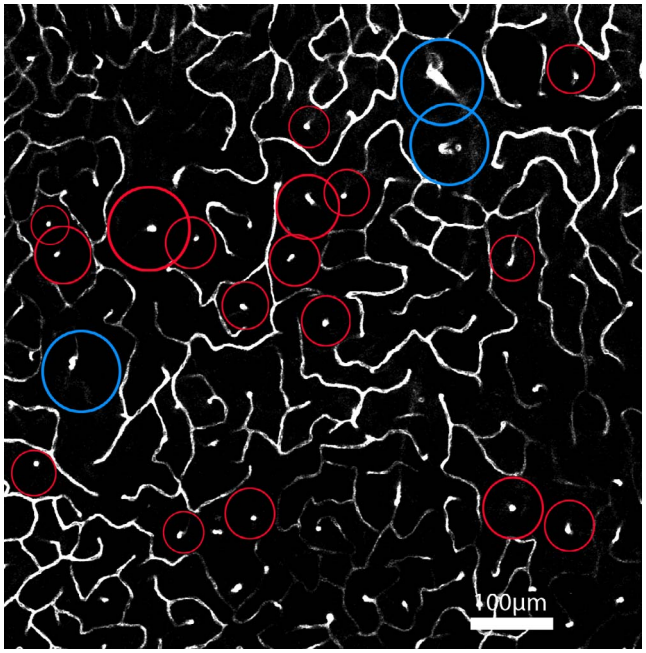

FIGURE 4. Examples of capillary-free areas in the IVP around capillaries bound to the DVP (*red circles*) and transverse veins emerging from the DVP (*blue circles*).

function of the size of Krogh's cylinder. In the IVP, we found a regular pattern of vessel distribution, regardless of the type of vessel (i.e., capillaries or venules). The capillary-free area was slightly higher around transverse venules than around capillaries. This suggested that there is a larger Krogh cylinder around transverse venules than around capillaries, and, hence, that veins also significantly participate in the physiologic delivery of oxygen to the retina.

Considering that most of the blood flow transits from the SVP to the CVP, the average length of retinal capillary pathway of red cells then could be evaluated. This can be estimated by adding successive vascular connected segments from precapillary arterioles to transverse venules, considering that capillaries go through half the length of the SVP, half the width of a watershed, half the average length of meandering venules, half the average length of a, RPC, half the width of a watershed in the DVP, and, finally, twice the distance between the SVP and the DVP. This estimate, which is conservative since it does not take into account the distance between the RPC and the DVP, suggests that the average length of the red cell pathway through the retina is at least in the range of 500 µm to 1 mm. This rather long pathway may participate in the high coefficient of extraction of oxygen in retinal vessels.[1]

The neural consequences of local hypoxia in the retina may be deduced from the Krogh's cylinders concept; that is, the more distant a neuron is from its source of oxygen, the more likely it is to be affected by decreased plasma oxygen

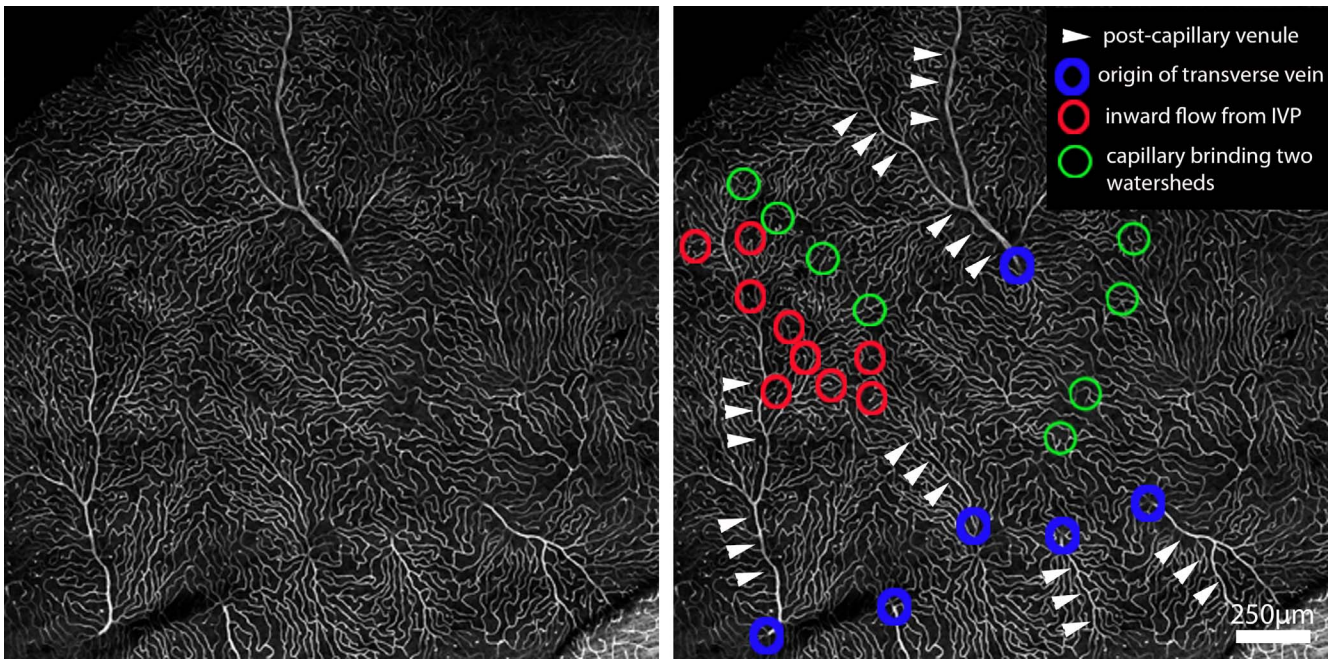

FIGURE 5. *Left*, wide field of the DVP. *Right*, annotations of microvascular structures.

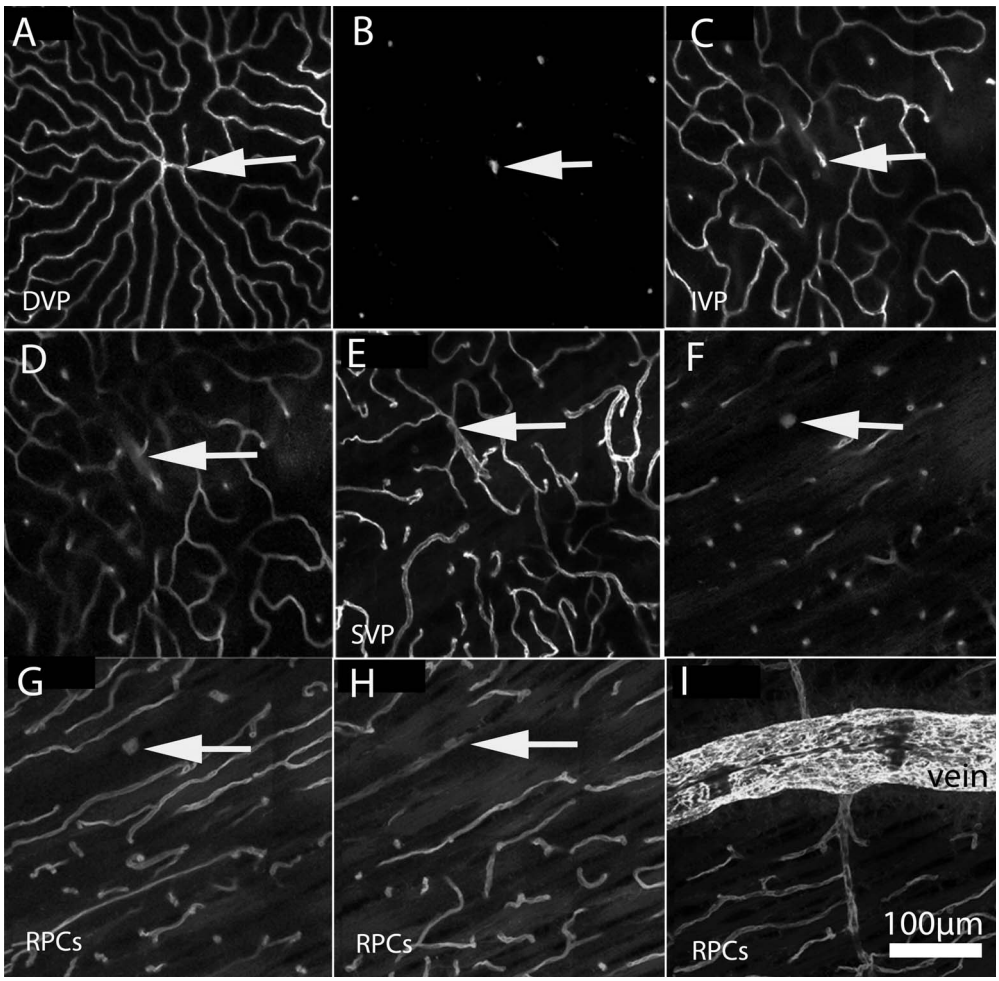

FIGURE 6. From (**A**) to (**I**), a collecting venule (*arrows* on successive images) is followed from the DVP (**A**) to a major vein (**I**) throughout the retinal vasculature.

Investigative Ophthalmology & Visual Science

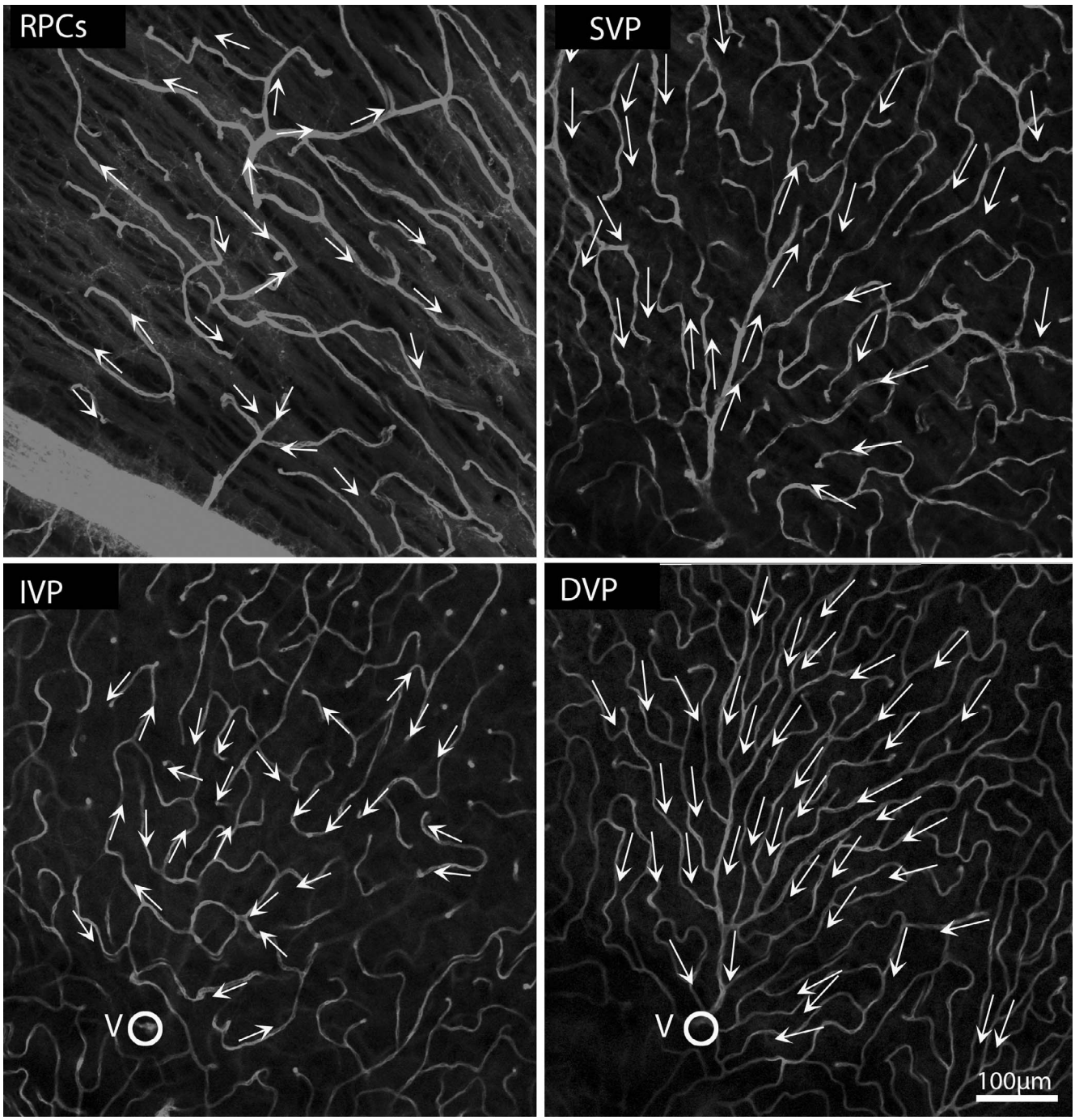

Figure 7. Example of the directions of capillary blood flow in each layer according to capillary connections.

saturation. Hence, in case of decreased blood flow without obstruction, hypoxia (and, hence, ischemia) will affect mostly the outer plexiform and inner nuclear layers around collecting venules (i.e., the area most distant from arterioles). Perivenular whitening,[25,26] also called paracentral acute middle maculopathy,[27,28] is a fundus feature encountered during acute central retinal vein occlusion. The serial organization of retinal layers provides a straightforward explanation for the localization of perivenular whitening in the DVP.[29–31] Indeed, there is angiographic evidence that the latter presentation is linked to panretinal hypoperfusion,[32] that is, severely impaired arterial inflow leading to a premature oxygen desaturation in precapillary arterioles. Our model suggested that perivenular whitening is initiated and/or more severe at the origin of draining venules (i.e., in the center of watersheds). Therefore, it may be predicted that the earliest spots of perivenular whitening are located around transverse venules. For the same reasons, this model also may explain why the NFL is relatively protected against global, subacute ischemia, such as that seen during carotid artery occlusion.[29]

This model also may be able to predict the consequences of a focal microvascular obstruction, such as embolic occlusion of a precapillary arteriole in the SVP. This will lead to ischemia of the neurons that are tributaries of the SVP; that is, the inner

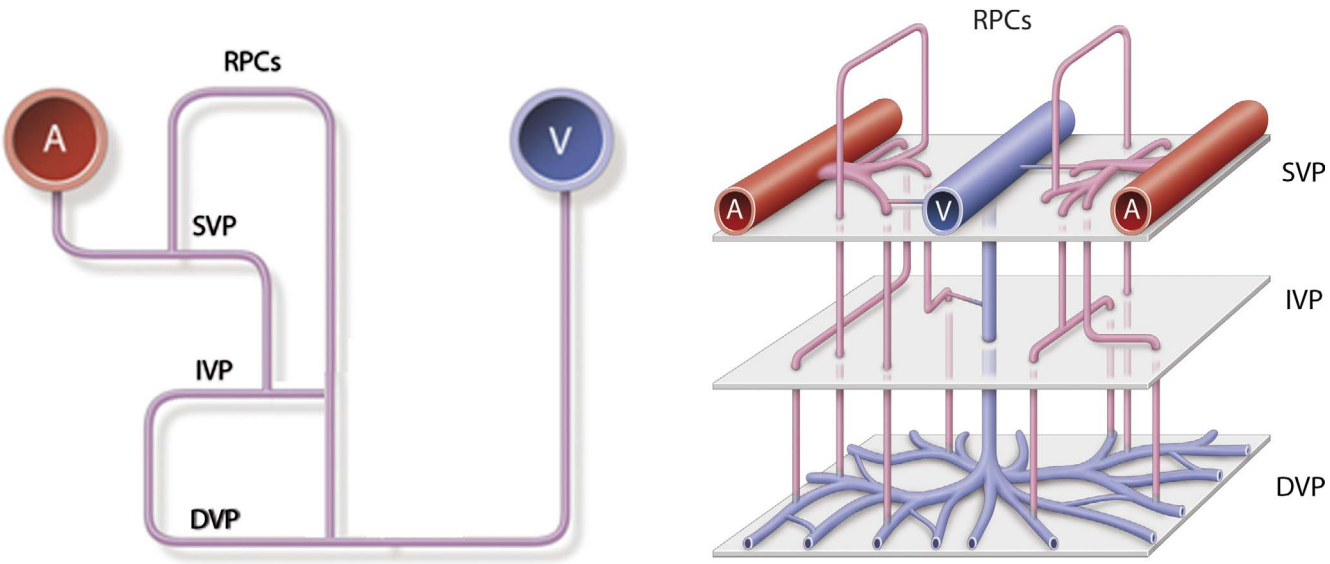

Figure 8. Proposed 2D and 3D models of the retinal microcirculation in the pig retina close to the optic disc.

plexiform layer and part of the inner nuclear layer, but is likely to have less effect on innermost and outermost neurons (i.e., those around the RPCs and DVP); indeed, the highly anastomotic capillaries in the RPCs and DVP may render them resilient to a focal SVP obstruction.

The DVP may be involved electively in vascular inflammation. It is known that diapedesis of blood-borne inflammatory cells occurs preferentially at postcapillary venules. The DVP has been shown to be involved in several models of retinal inflammation, yet not at the earliest phase.[33–35] A peculiar case is represented by experimentally-induced cerebral malaria in mice in which inflammatory changes in retinal vessels were confined on the venous side of the inner vasculature.[36] Taken together, these findings suggest a model in which the earliest site of experimental inflammation is in venules of the SVP, and with time and severity there is posterior extension of inflammatory changes, possibly along the collecting venules down to the DVP. Hence, assessing the involvement of collecting venules during experimentally-induced retinal inflammation may be of interest to understand how does the inflammation propagates from inner to outer retina.

After a branch retinal vein occlusion (BRVO), the development of shunt vessels deriving venous blood from one territory to neighboring ones is observed commonly. The rich anastomotic network in the DVP provides an obvious escape pathway for the obstructed venous flow, that is, from one watershed to its neighboring ones. Accordingly, following BRVO, collateral vessels develop electively in the DVP in rats[6] and humans.[37] These collaterals probably develop from the dilation of capillaries at the borders of watersheds, which transfer the venous flow from obstructed to neighboring watersheds. Because the DVP is anastomotic throughout the retina, it, therefore, is likely that a BRVO may affect the flow of the DVP over a larger area than that of the watershed directly affected by the venous obstruction. It would be of interest to analyze if the aspect of the DVP already is altered in presence of pathologic arteriovenous crossings, which theoretically may be compensated by redirection of the flow of the DVP toward adjacent watersheds.

Finally, the direct connections of the SVP to major veins (i.e., shunting the IVP and DVP) provides a potential site for the adaptation of blood flow to local demand. The permeability of these capillaries, indeed, may modulate the proportion of flow directed toward the RPCs and DVP. Interestingly, elective nonperfusion of the DVP has been reported during diabetic retinopathy,[38,39] which may be due to dysregulation of the conductance of these shunting capillaries. This also raises an interesting hypothesis regarding the cause of the worse prognosis of RVO in diabetics,[40] since the loss of the DVP capillaries due to diabetic microvasculopathy may diminish consecutively the capability shunt vessels to develop in the DVP.

Potential limits of this work are the small sampling, which limits the determination of average microvascular densities, the absence of unequivocal determination of the nature of microvessels, and the fact that the estimation of blood flow repartition assumes equal conductance for each capillary. Our model, despite its limitations, may nevertheless provide a scaffold for the interpretation of blood flow analysis in humans.

Further investigations of the relationship between neuronal and vascular organization are of interest. In particular, it would be interesting to determine to which extent the distribution of photoreceptor synapses determines the distribution of capillaries in the DVP; it can be hypothesized that the cone synapses would be closer to capillaries than rod synapses due to their higher metabolic demand. Another interesting consequence of our work is that numerical models of flow conductance and shear stress may be extended to microvessel layers.[41]

Acknowledgments

Supported by the Institut National de la Santé et de la Recherche Médicale (Contrat d'Interface 2011) and the Agence Nationale de la Recherche (ANR-12-TECS-0015-03, LabEx LIFESENSES ANR-10-LABX-65, ANR-11-IDEX-0004-02). The authors alone are responsible for the content and writing of this paper.

Disclosure: **S. Fouquet**, None; **O. Vacca**, None; **F. Sennlaub**, None; **M. Paques**, None

References

1. Linsenmeier RA, Zhang HF. Retinal oxygen: from animals to humans. *Prog Retin Eye Res*. 2017;58:115–151.

2. Tick S, Rossant F, Ghorbel I, et al. Foveal shape and structure in a normal population. *Invest Ophthalmol Vis Sci*. 2011;52: 5105–5110.
3. Samara WA, Say EA, Khoo CT, et al. Correlation of foveal avascular zone size with foveal morphology in normal eyes using optical coherence tomography angiography. *Retina*. 2015;35:2188–2195
4. Snodderly DM, Weinhaus RS, Choi JC. Neural-vascular relationships in central retina of macaque monkeys (macaca fascicularis). *J Neurosci*. 1992;12:1169–1193.
5. Henkind P. Radial peripapillary capillaries of the retina. I. Anatomy: human and comparative. *Br J Ophthalmol*. 1967; 51:115–123.
6. Paques M, Tadayoni R, Sercombe R, et al. Structural and hemodynamic analysis of the mouse retinal microcirculation. *Invest Ophthalmol Vis Sci*. 2003;44:4960–4967.
7. Genevois O, Paques M, Simonutti M, et al. Microvascular remodeling after occlusion-recanalization of a branch retinal vein in rats. *Invest Ophthalmol Vis Sci*. 2004;45:594–600.
8. Simoens P, De Schaepdrijver L, Lauwers H. Morphologic and clinical study of the retinal circulation in the miniature pig. A: morphology of the retinal microvasculature. *Exp Eye Res*. 1992;54:965–973.
9. Foreman DM, Bagley S, Moore J, Ireland GW, McLeod D, Boulton ME. Three dimensional analysis of the retinal vasculature using immunofluorescent staining and confocal laser microscopy. *Br J Ophthalmol*. 1996;80:246–251.
10. Tan PE, Yu PK, Balaratnasingam C, et al. Quantitative confocal imaging of the retinal microvasculature in the human retina. *Invest Ophthalmol Vis Sci*. 2012;53:5728–5736.
11. Yu PK, Balaratnasingam C, Cringle SJ, et al. Microstructure and network organization of the microvasculature in the human macula. *Invest Ophthalmol Vis Sci*. 2010;51:6735–6743.
12. Rootman J. Vascular system of the optic nerve head and retina in the pig. *Br J Ophthalmol*. 1971;55:808–819.
13. Weinhaus RS, Burke JM, Delori FC, et al. Comparison of fluorescein angiography with microvascular anatomy of macaque retinas. *Exp Eye Res*. 1995;61:1–16.
14. Pinhas A, Dubow M, Shah N, et al. In vivo imaging of human retinal microvasculature using adaptive optics scanning light ophthalmoscope fluorescein angiography. *Biomed Opt Express*. 2013;4:1305–1317.
15. Spaide RF, Klancnik JM Jr, Cooney MJ. Retinal vascular layers imaged by fluorescein angiography and optical coherence tomography angiography. *JAMA Ophthalmol*. 2015;133:45–50.
16. Kurokawa K, Sasaki K, Makita S, Hong Y-J, Yasuno Y. Three-dimensional retinal and choroidal capillary imaging by power Doppler optical coherence angiography with adaptive optics. *Opt Express*. 2012;20:22796–22812.
17. Bonnin S, Mané V, Couturier A, et al. New insight into the macular deep vascular plexus imaged by optical coherence tomography angiography. *Retina*. 2015;35:2347–2352.
18. Coscas F, Sellam A, Glacet-Bernard A, et al. Normative data for vascular density in superficial and deep capillary plexuses of healthy adults assessed by optical coherence tomography angiography. *Invest Ophthalmol Vis Sci*. 2016; 57:211–223.
19. Campbell JP, Zhang M, Hwang TS, et al. Detailed vascular anatomy of the human retina by projection-resolved optical coherence tomography angiography. *Sci Rep*. 2017;7: 42201
20. Savastano MC, Lumbroso B, Rispoli M. In vivo characterization of retinal vascularisation morphology using optical coherence angiography. *Retina*. 2015;35:2196–2203.
21. Zhang M, Hwang TS, Campbell JP, et al. Projection-resolved optical coherence tomographic angiography. *Biomed Opt Express*. 2016;7:816–828.
22. Gorczynska I, Migacz JV, Zawadzki RJ, Capps AG, Werner JS. Comparison of amplitude-decorrelation, speckle-variance and phase-variance OCT angiography methods for imaging the human retina and choroid. *Biomed Opt Express*. 2016;7: 911–942.
23. Birol G, Wang S, Budzynski E, Wangsa-Wirawan ND, Linsenmeier RA. Oxygen distribution and consumption in the macaque retina. *Am J Physiol Heart Circ Physiol*. 2007; 293:H1696–H1704.
24. Emmenlauer M, Ronneberger O, Ponti A, et al. XuvTools: free, fast and reliable stitching of large 3D datasets. *J Microsc*. 2009:233:42–60.
25. McLeod D. Krogh cylinders in retinal development, panretinal hypoperfusion and diabetic retinopathy. *Acta Ophthalmol*. 2010;88:817–835.
26. Paques M, Gaudric A. Perivenous macular whitening during central retinal vein occlusion. *Arch Ophthalmol*. 2003;121: 1488–1491.
27. Sarda V, Nakashima K, Wolff B, Sahel JA, Paques M. Topography of patchy retinal whitening during acute perfused retinal vein occlusion by optical coherence tomography and adaptive optics fundus imaging. *Eur J Ophthalmol*. 2011;21:653–656.
28. Browning DJ. Patchy ischemic retinal whitening in acute central retinal vein occlusion. *Ophthalmology*. 2002;109: 22154–22159.
29. Chen X, Rahimy E, Segott RC, et al. Spectrum of retinal vascular disease associated with paracentral acute middle maculopathy. *Am J Ophthalmol*. 2015;160:26–34.
30. Sarraf D, Rahimy E, Fawzi AA, et al. Paracentral acute middle maculopathy: a new variant of acute macular neuroretinopathy associated with retinal capillary ischemia. *JAMA Ophthalmol*. 2013;13:1275–1287.
31. Falavarjani KG, Phasukkijwatana N, Cunningham ET, et al. En face OCT analysis to assess the spectrum of perivenular ischemia and paracentral acute middle maculopathy in retinal vein occlusion. *Am J Ophthalmol*. 2017;177:131–138.
32. Paques M, Baillart O, Genevois O, Gaudric A, Lévy BI, Sahel J. Systolodiastolic variations of blood flow during central retinal vein occlusion: exploration by dynamic angiography. *Br J Ophthalmol*. 2005;89:1036–1040.
33. Hu P, Pollard JD, Chan-Ling T. Breakdown of the blood-retinal barrier induced by activated T cells of nonneural specificity. *Am J Pathol*. 2000;156:1139–1149.
34. Xu H, Forrester JV, Liversidge J, Crane IJ. Leukocyte trafficking in experimental autoimmune uveitis: breakdown of blood-retinal barrier and upregulation of cellular adhesion molecules. *Invest Ophthalmol Vis Sci*. 2003;44:226–234
35. Xu H, Dawson R, Crane IJ, Liversidge J. Leukocyte diapedesis in vivo induces transient loss of tight junction protein at the blood-retina barrier. *Invest Ophthalmol Vis Sci*. 2005;46: 2487–2494.
36. Ma N, Hunt NH, Madigan MC, Chan-Ling T. Correlation between enhanced vascular permeability, up-regulation of cellular adhesion molecules and monocyte adhesion to the endothelium in the retina during the development of fatal murine cerebral malaria. *Am J Pathol*. 1996;149:1745–1762.
37. Suzuki N, Hirano Y, Yoshida M, et al. Microvascular abnormalities on optical coherence tomography angiography in macular edema associated with branch retinal vein occlusion. *Am J Ophthalmol*. 2016;161:126–132.

Investigative Ophthalmology & Visual Science

38. Couturier A, Mané V, Bonnin S, et al. Capillary plexus anomalies in diabetic retinopathy on optical coherence tomography angiography. *Retina*. 2015;35:2384–2391.
39. Park JJ, Soetikno BT, Fawzi AA. Characterization of the middle capillary plexus using optical coherence tomography angiography in healthy and diabetic eyes. *Retina*. 2016;36:2039–2050.
40. The Central Vein Occlusion Study Group. Natural history and clinical management of central retinal vein occlusion. *Arch Ophthalmol*. 1997;115:486–491
41. Ganesan P, He S, Xu H. Analysis of retinal circulation using an image-based network model of retinal vasculature. *Microvasc Res*. 2010;80:99–109.

Investigative Ophthalmology & Visual Science